https://dx.doi.org/10.4314/dujopas.v9i4a.9
ISSN (Print): 2476-8316
ISSN (Online): 2635-3490
Dutse Journal of Pure and Applied Sciences (DUJOPAS), *Vol. 9 No. 4a December 2023*

Application of Geophysical Methods for Investigation of Groundwater Potential in Layunrun Village, Ogun State, Southwestern Nigeria

J. O. Airen*[1] , J. O. Osifo[1]

[1]Department of Physics,
Faculty of Physical Sciences,
University of Benin,
Benin City,
Nigeria

Email: osariere.airen@uniben.edu

Abstract

An investigation of the groundwater potential of the area for tube well construction has been conducted in Layunrun village in a typical basement complex of Ogun State using electromagnetic and electrical resistivity techniques in geophysical exploration. Six (6) electromagnetic profiles were used, and twenty-eight (28) Vertical Electrical Soundings (VES) were performed along some of the profiles' potential regions. The typical partial curve matching utilized to create the VES curves was examined, and the results were used to create themed maps of the region. Within the study area, between four and six geoelectric layers were found. These layers are Topsoil, weathered layer (clay), weathered layer, fractured basement, and fresh basement. According to the findings, a bigger percentage of the land has an overburden thickness ranging from 9 to 17 m, with a maximum overburden of about 23 m. It also showed how well fractured the research area is, with thicknesses of the fractures varying from about 12 m to more than 30 m. The study area has a good chance of accumulating groundwater and, consequently, developing groundwater through digging boreholes. The outcomes also suggested that a community with similar geological settings may use the electromagnetic method in addition to the electrical resistivity method to identify places with high groundwater potentials.

Keywords: Geophysical methods, groundwater potential, weathered layer, basement, borehole

INTRODUCTION

The availability of a reliable and sustainable water supply is crucial for agricultural activities in order to ensure optimal crop growth and productivity. Farms located in places with restricted access to surface water supplies depend heavily on boreholes, also known as tube wells (Madramootoo *et al.*, 2018). However, boreholes may experience several problems with time, including decreased water yield, poor water quality, and even total failure. Crop loss, a decline in agricultural output, and financial losses for farmers are all possible effects of a failed borehole in a farm. Restoring the water supply and ensuring the farm's continuing operation depends on identifying the reasons for borehole failure and implementing adequate remediation procedures. Visual examination and manual measurements are time-consuming, irrational and may not provide comprehensive information about the subsurface conditions in failed drilling investigations using traditional methods (Saha *et al.*, 2019). Integrating

---

*Author for Correspondence

geophysical approaches has drawn a lot of attention recently as a way to get around these constraints.

The electrical resistivity method and the electromagnetic (EM) approach are two widely utilized geophysical techniques for subsurface research. In contrast to the electrical resistivity approach, which evaluates the electrical resistance of subsurface materials, the EM method uses measurements of electromagnetic fields to characterize subsurface properties (Yan and Zhang, 2016). The combination of these two geophysical techniques offers a thorough and complementary strategy for determining the reasons for borehole failure. According to Minsley *et al*. (2015), the EM technique aids in locating potential fractures or cavities that are filled with water and offers information on the presence of conductive materials (such as water-bearing formations). As opposed to this, the electrical resistivity approach aids in identifying subsurface differences in resistivity, which may point to lithological changes, the existence of groundwater, or regions with increased permeability (Kumar *et al.,* 2018). In earlier research, the merging of the electromagnetic and electrical resistivity approaches in the analysis of failed boreholes in agricultural contexts showed encouraging results. For instance, Saha *et al.,* 2019, used a case study of a botched geophysical drilling investigation to show the value of combining electromagnetic and electrical resistivity approaches when describing subsurface conditions. Their results demonstrated the benefits of these integrated methodologies in pinpointing the root reasons for borehole failure and offering useful data for rehabilitation plans.

Saha *et al.,* 2019, used a case study of a botched geophysical drilling investigation to show the value of combining electromagnetic and electrical resistivity approaches when describing subsurface conditions. Their results demonstrated the benefits of these integrated methodologies in pinpointing the root reasons for borehole failure and offering useful data for rehabilitation plans.

Farmers, water resource managers, and other agricultural stakeholders will need to consider the practical consequences of this study's findings. The study will contribute to the improvement of approaches for diagnosing and mitigating borehole failures in agricultural settings by comprehending the reasons for borehole failure and adopting efficient rehabilitation procedures. The end result will be an improvement in water resource management, the promotion of sustainable farming methods, and the guarantee of a sustainable and stable water supply for agricultural activities. The subsurface conditions surrounding a failed borehole in a farm can be better understood by researchers and practitioners by combining the EM and electrical resistivity methods. By using an integrated approach, they may evaluate hydraulic connectivity, locate preferential flow patterns, identify potential sources of pollution, and decide on the best places to drill new wells or repair existing ones.

MATERIALS AND METHODS

Geological Setting of the Study Area

The study area is located at Layunrun Village, Abeokuta in which Abeokuta is a Basement complex. The site lies between latitude 7^{0} 08′ 23.78″ N to 7^{0} 08′ 27.43″ N, and longitude 3^{0} 41′ 17.61″ E to 3^{0} 41′ 20.86″ E with an approximate area spread of 556.2 km^{2}. Layunrun Village is located in Obafemi Owode Local Government area of Ogun State (Figure 1).

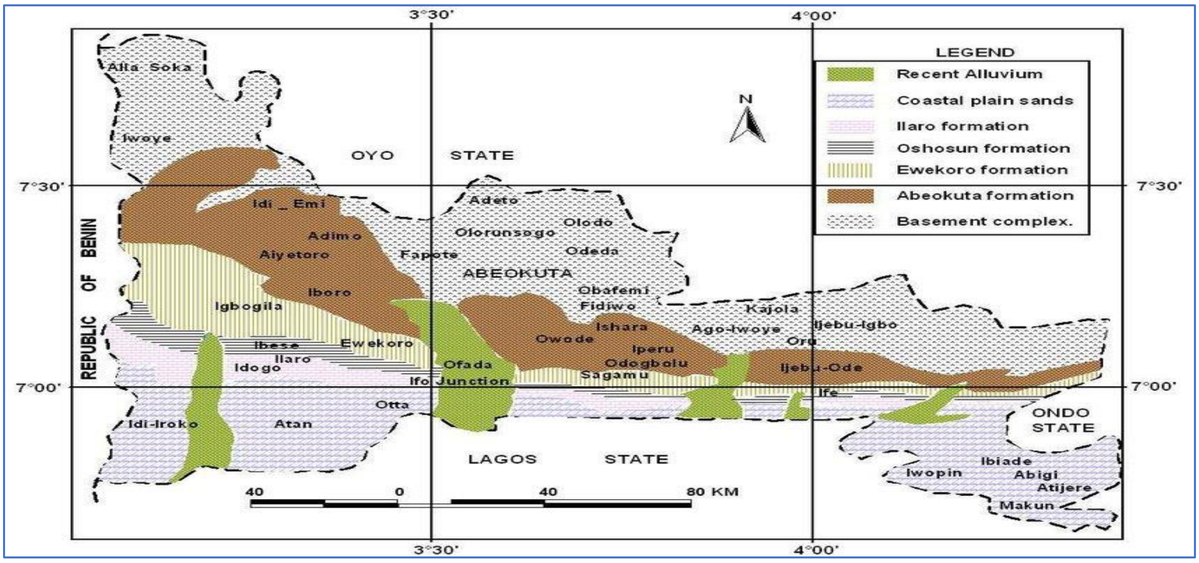

Figure 1: Geological map showing the study area

Layunrun, Abeokuka, according to its geology, is part of the Abeokuta group, which is part of the Basement complex terrain of the Dahomey Basin (Agagu, 1985). According to Ariyo and Adeyemi (2012), this formation displays the lithologies of sandstones, gritstones, siltstones, limestones, shales, and sands. Figures 1 and 2, respectively, display the extracted geology and the study area's basemap.

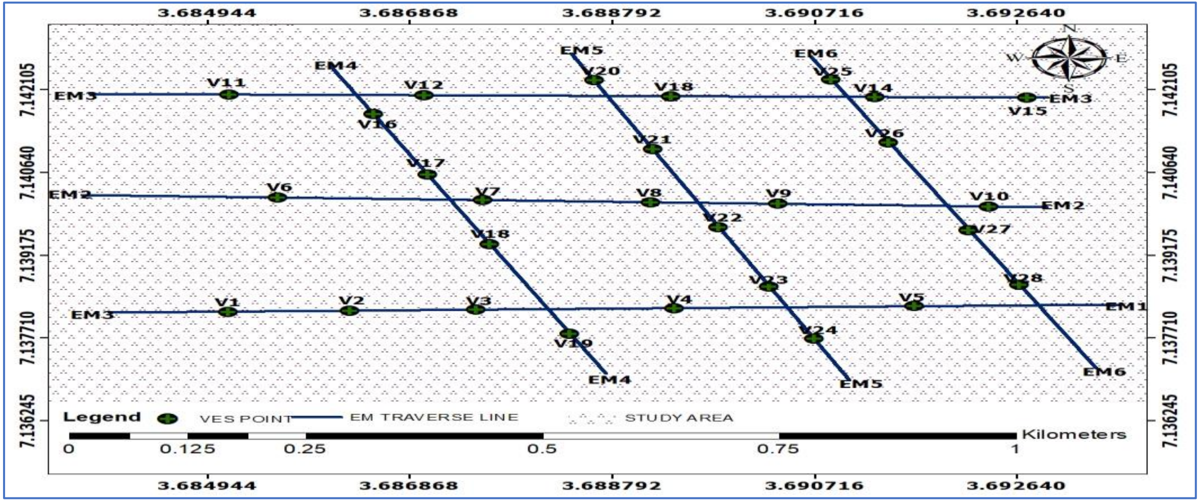

Figure 2: Basemap of the study area

Vertical Electrical Sounding (VES) and electromagnetic (EM) geophysical techniques were used in this study. The PASI earth resistivity meter 16GL model was used to collect resistivity data while the EM survey was conducted using the EM34-3 Geonics instrument.

According to Bhattacharya and Patra (1968), VanNorstrand and Cook (1966), Ritz *et al.* (1999), the electrical resistivity approach involves measuring the potential at the surface that arises from a known current flowing into the ground. The electrodes utilized are a pair of potential electrodes, M and N, and a pair of current electrodes, A and B. Equation 1 yields the apparent resistivity, where a.

$$\rho_a = \frac{K\Delta V}{I} \qquad (1)$$

where V stands for the observed potential difference, I for current intensity, and K for a geometric coefficient based on the electrode array. The ERI approach uses a multi-core cable with as many electrodes inserted into the ground at preset intervals, in accordance with a set of predefined readings stored in the equipment's internal memory. The mixed sounding is made up of several configurations of transmitting (A, B) and receiving (M, N) pairs of electrodes, with a maximum investigation depth that mostly depends on the length of the cable (Figure 3). The spatial resolution and depth of analysis in electrical resistivity methods are correlated with the distance between electrodes.

For Schlumberger array, the greatest depth of examination, as a preliminary guess, is in the range of 20% d for the Schlumberge

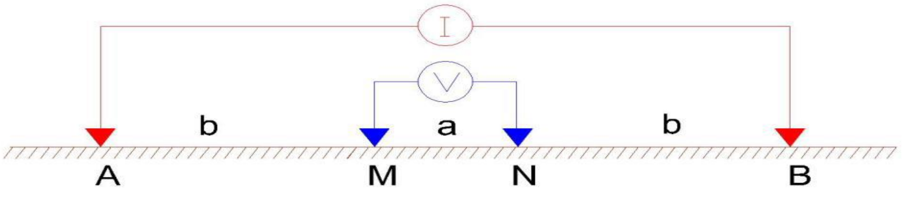

Figure 3: Electrc

A. Data Acquisition

Data from the Vertical Electrical Sounding (VES) acquisition were analyzed quantitatively and qualitatively. The partial curve matching technique was employed for the quantitative interpretation of the depth-sounding curves (Bhattacharya and Patra, 1968). To do this, a translucent piece of paper was used to map the VES data.

Inducing and detecting current flow in geological formations is based on the physical principles of the electromagnetic approach. The total conductivity of the subsurface is measured electromagnetically (it is the inverse of resistivity). To express the conductivity of electromagnetic measurements, the units milliphos/meter (pronounced "milli-mohs per meter") or millisemenes/meter, mS/m (1 milliphos = 1 millisemenes, mS), are commonly used. The opposite of "Mho" is "ohm."

B. Data Processing

In the partial curve matching method, two (2) standard master curve layers and four (4) auxiliary type curves (H, K, A, and Q) were used. To complete this method, it was necessary to match the curve segments one by one, beginning at the place with the shortest electrode spacing and moving in the opposite direction. Following the partial curve matching, the VES curve results were used to confine the interpretation by a computer-assisted inversion. The overestimation of depths in the curve matching is always decreased by doing this. The computer's iterative process produces a quantitative analysis that reveals the resistivity, thickness, and depth.

Alternating current is passed through a wire coil (the transmitter) to create an electromagnetic field. The magnetic component of the EM wave causes eddy currents (AC) in conductive materials in the ground if there are any. According to Klein and Lajoie (1980), eddy currents generate secondary EM fields that a receiver can pick up on. The primary field is also picked up by the receiver, and the combined field is made up of secondary fields that are different from the primary field in terms of amplitude and phase. With the use of some simplifying presumptions, the phase-shifted component (or quadrature) can be transformed into a gauge of apparent ground conductivity.

RESULTS AND DISCUSSION

The VES data results are depicted in Figure 4 as well. The findings demonstrate the presence of QHA, QA, QH, HA, and QHKH-type curves in the studied area. The fact that QHA-type curves make up 85.7% of the area and the other type curves make up just 3.57% of the area per each further demonstrates this. Table 1 provides a summary of the findings.

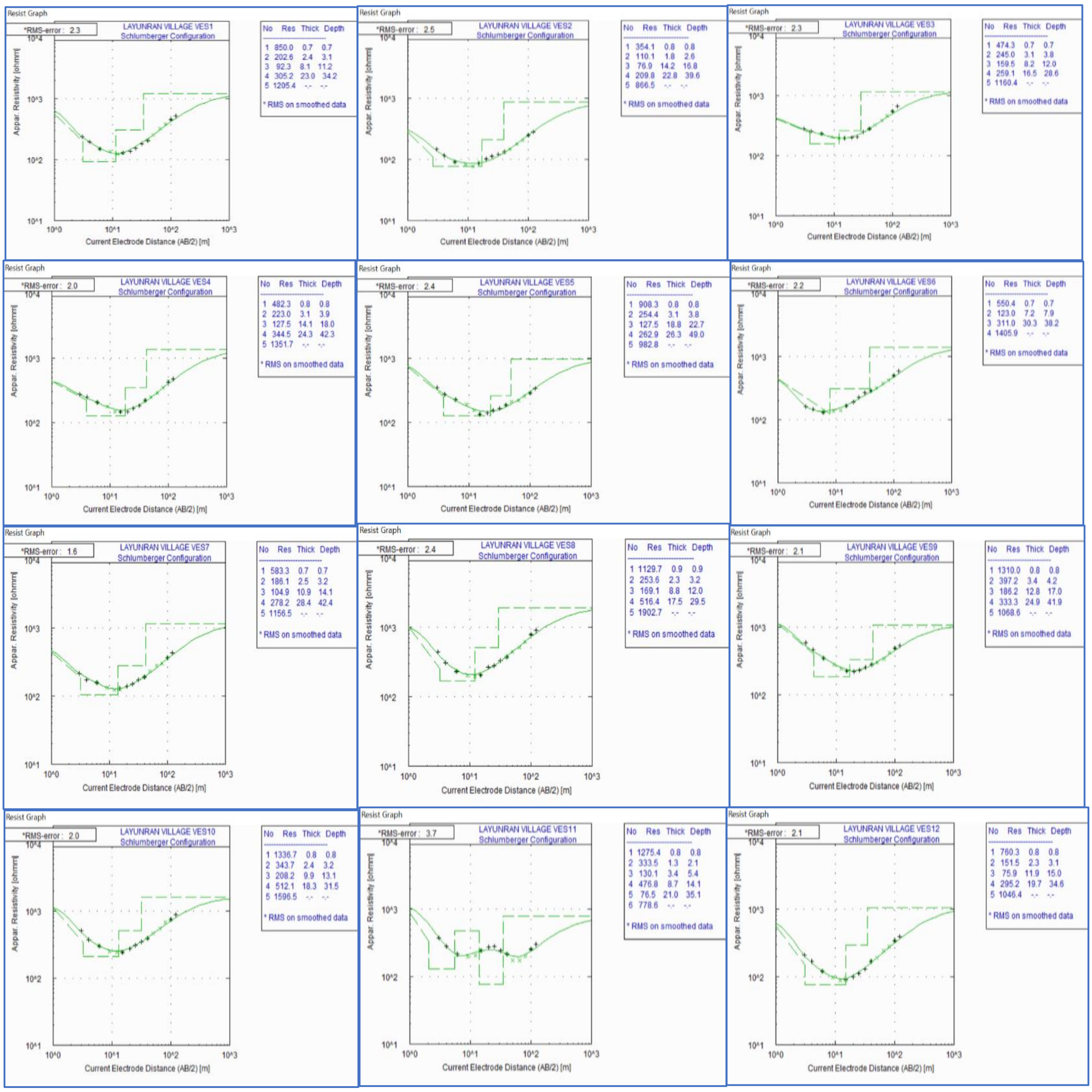

LAYUNRAN VILLAGE VES1
Schlumberger Configuration
*RMS-error : 2.3

No	Res	Thick	Depth
1	850.0	0.7	0.7
2	202.6	2.4	3.1
3	92.3	8.1	11.2
4	305.2	23.0	34.2
5	1205.4	-.-	-.-

* RMS on smoothed data

LAYUNRAN VILLAGE VES2
Schlumberger Configuration
*RMS-error : 2.5

No	Res	Thick	Depth
1	354.1	0.8	0.8
2	110.1	1.8	2.6
3	76.9	14.2	16.8
4	209.8	22.8	39.6
5	866.5	-.-	-.-

* RMS on smoothed data

LAYUNRAN VILLAGE VES3
Schlumberger Configuration
*RMS-error : 2.3

No	Res	Thick	Depth
1	474.3	0.7	0.7
2	245.0	3.1	3.8
3	159.5	8.2	12.0
4	259.1	16.5	28.6
5	1160.4	-.-	-.-

* RMS on smoothed data

LAYUNRAN VILLAGE VES4
Schlumberger Configuration
*RMS-error : 2.0

No	Res	Thick	Depth
1	482.3	0.8	0.8
2	223.0	3.1	3.9
3	127.5	14.1	18.0
4	344.5	24.3	42.3
5	1351.7	-.-	-.-

* RMS on smoothed data

LAYUNRAN VILLAGE VES5
Schlumberger Configuration
*RMS-error : 2.4

No	Res	Thick	Depth
1	908.3	0.8	0.8
2	254.4	3.1	3.8
3	127.5	18.8	22.7
4	262.9	26.3	49.0
5	982.8	-.-	-.-

* RMS on smoothed data

LAYUNRAN VILLAGE VES6
Schlumberger Configuration
*RMS-error : 2.2

No	Res	Thick	Depth
1	550.4	0.7	0.7
2	123.0	7.2	7.9
3	311.0	30.3	38.2
4	1405.9	-.-	-.-

* RMS on smoothed data

LAYUNRAN VILLAGE VES7
Schlumberger Configuration
*RMS-error : 1.6

No	Res	Thick	Depth
1	583.3	0.7	0.7
2	186.1	2.5	3.2
3	104.9	10.9	14.1
4	278.2	28.4	42.4
5	1156.5	-.-	-.-

* RMS on smoothed data

LAYUNRAN VILLAGE VES8
Schlumberger Configuration
*RMS-error : 2.4

No	Res	Thick	Depth
1	1129.7	0.9	0.9
2	253.6	2.3	3.2
3	169.1	8.8	12.0
4	516.4	17.5	29.5
5	1902.7	-.-	-.-

* RMS on smoothed data

LAYUNRAN VILLAGE VES9
Schlumberger Configuration
*RMS-error : 2.1

No	Res	Thick	Depth
1	1310.0	0.8	0.8
2	397.2	3.4	4.2
3	186.2	12.8	17.0
4	333.3	24.9	41.9
5	1068.6	-.-	-.-

* RMS on smoothed data

LAYUNRAN VILLAGE VES10
Schlumberger Configuration
*RMS-error : 2.0

No	Res	Thick	Depth
1	1336.7	0.8	0.8
2	343.7	2.4	3.2
3	208.2	9.9	13.1
4	512.1	18.3	31.5
5	1596.5	-.-	-.-

* RMS on smoothed data

LAYUNRAN VILLAGE VES11
Schlumberger Configuration
*RMS-error : 3.7

No	Res	Thick	Depth
1	1275.4	0.8	0.8
2	333.5	1.3	2.1
3	130.1	3.4	5.4
4	476.8	8.7	14.1
5	76.5	21.0	35.1
6	778.6	-.-	-.-

* RMS on smoothed data

LAYUNRAN VILLAGE VES12
Schlumberger Configuration
*RMS-error : 2.1

No	Res	Thick	Depth
1	760.3	0.8	0.8
2	151.5	2.3	3.1
3	75.9	11.9	15.0
4	295.2	19.7	34.6
5	1046.4	-.-	-.-

* RMS on smoothed data

Figure 4: Typical Type Curves of the Study Area

Five maps (Figures 5, 6 and 7) were generated from the results of the VES. These include the overburden thickness map, fracture thickness map, fracture Isoresistivity, basement Isoresistivity and basement topography maps.

Table 1. Summary of Interpreted VES (1 to 28) results

Resistivity (Ωm)	Thickness (m)	Depth (m)	Lithology
331.8 – 3694.2	0.6 – 1.0	0.6 – 1.0	Topsoil
58.5 – 732.5	1.3 – 14.2	2.6 – 19.2	Weathered layer
21.8	8.3	12.4	Weathered layer (Clay)
100.5 – 522.0	8.7 – 28.4	14.1 – 49.0	Fractured Basement
778.6 – 2722.9	---	---	Fresh Basement

The VES consists of four to six geoelectric layers, denoted as VES 1 to 28. These layers correspond to specific subsurface formations, including the topsoil, a clayey weathered layer, a deeper weathered layer, a fractured basement, and a fresh basement.

The uppermost layer, referred to as the topsoil, is the first horizon encountered in VES data. This layer exhibits resistivity values ranging from 331.8 to 3694.2 ohm-m, with a thickness varying between 0.6 and 1.0 meters. Moving deeper into the subsurface, the second geoelectric layer consistently identified across VES 1 to 28 is the weathered layer. This layer is characterized by resistivity values spanning from 110.1 to 735.5 ohm-m and exhibits a thickness ranging from 1.3 to 4.0 meters.

In VES profiles 1 to 5, 7 to 22, and 24 to 27, the third geoelectric layer is indicative of another weathered layer. This layer is recognized by resistivity values ranging from 58.5 to 208.2 ohm-m and thicknesses spanning from 3.4 to 18.8 meters.
However, in VES profiles 6 and 23, the third layer displays distinct characteristics, including resistivity values ranging from 311.0 to 409.3 ohm-m and a thickness spanning from 16.0 to 30.3 meters, suggesting a fragmented basement.

In VES 28, the third layer stands out with a resistivity of 21.8 ohm-m and a thickness of 8.3 meters, resembling a weathered layer, particularly clay. The fourth layer identified in VES profiles 1 to 5, 7 to 17, 19 to 22, and 24 to 28 is characterized by resistivity values ranging from 100.5 to 522.0 ohm-m and thicknesses ranging from 8.7 to 28.4 meters, indicating a fragmented basement.

In contrast, VES profiles 6, 18, and 23 exhibit different resistivity readings within the fourth layer, ranging from 1070.9 to 1405.9 ohm-m. While these readings suggest a new basement, the precise layer thickness in this zone could not be determined because the current ceased.

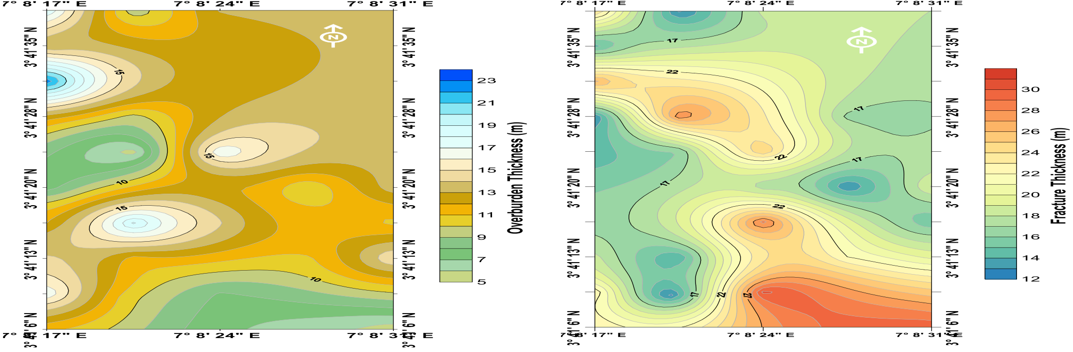

Figure 5: Map of the (a) Overburden thickness and (b) Fracture thickness of the study area.

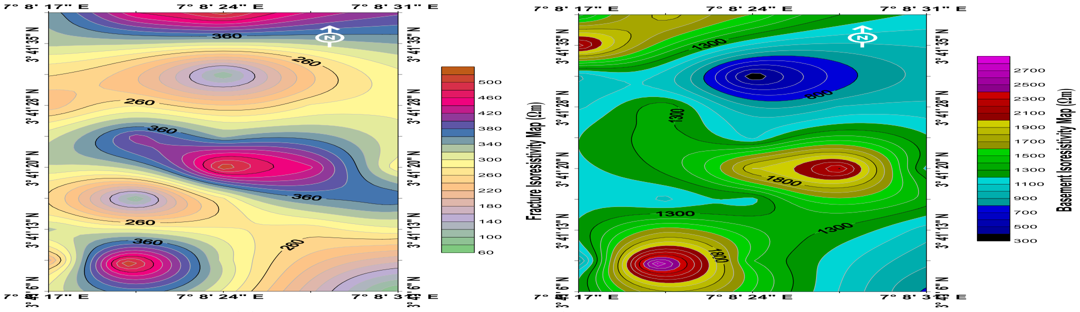

Figure 6: Map of the (a) Fracture Isoresistivity and (b) Basement Isoresistivity of the study area.

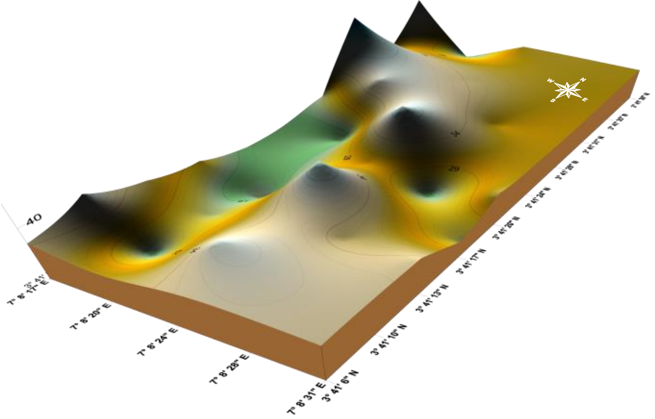

Figure 7: Basement Topography Map of the Study Area.

With resistivity values ranging from 866.5 to 2722.9 ohm-m, the fifth geologic unit in the VES (1 to 5, 7 to 10, 12 to 17, 19 to 22, and 24 to 27) is a sign of a new basement, although it was impossible to determine how thick its layers were because current terminated within this zone. The weathered layer and cracked foundation, with resistivity values of 76.5 ohm-m and 314.6 ohm-m, respectively, were discovered in the fifth horizon beneath VES (11 and 28). The layer thickness of VES 11 is 21.0 m, but it was unable to determine the layer thickness of VES 28 because current ended in this area. With a resistivity value of 778.6 ohm-m, the sixth horizon beneath VES 11 is indicative of a fresh basement, however, the thickness could not be determined because current terminated within this zone. The cracked zones in the VES show an aquifer unit that could be tapped into.

A. The Maps

The research area's overburden thickness is generally thin, with a maximum thickness of around 23 m indicated in the area's northwest, according to the overburden thickness map (Figure 6a). The chart also demonstrates that a bigger percentage of the area exhibits overburden thicknesses ranging from 9 to 17 m, while a much smaller fraction (the lower south-south and western regions) exhibits overburden thicknesses ranging from 5 to 9 m.

Faults, fractures, and joints are crucial geologic structures for groundwater accumulation because they can operate as conduits for regions of groundwater accumulation. The investigation's findings revealed that the studied area is extensively broken, with fracture thicknesses ranging from less than 12 meters to more than 30 meters (Figure 5b). The maximum fracture thicknesses were found in the research area's southeast, central, and northwest regions. The lower fracture thickness in the southwest and northeastern portions of the study region is on either side of this.

The fresh basement's isoresistivity map (Figure 6a), which lies underneath the research area, shows that the resistivity value was very variable. The northeastern zone showed the lowest resistivity (300 - 900 ohm-m), indicating that the rocks within this zone may be on the verge of weathering. The lower southwestern, eastern, and northwestern regions showed the highest resistivity (1900 - 2900 ohm-m), indicating that the rocks in these regions are really fresh.

The fractured column inside the study area contains a range of resistivity values, as demonstrated by the isoresistivity map of the fractured zone in (figure 6b). Except in the lower southwestern, central, and northern regions, where the resistivity values are higher and range from around 380 to 580 ohm-m, the resistivity values typically range from 60 to 340 ohm-m. The research region's basement topography (Figure 7) is undulating, with greater depressions in the western and central parts of the area. These depressions might act as areas where groundwater collects. According to the underlying geology, the depressions might be a sign of softer rock units in the western and central regions.

B. Electromagnetic Profiling along Traverses

Figure 8 (a and b) shows that the apparent conductivity along traverse (1 to 6) ranged from 16 to 145 mS/m for the electromagnetic profiling. Due to the low conductivity along these profiles, the bedrock may be rather close to the surface. However, high amplitude peck points were seen across the profiles at conductivity values of 85 mS/m on the horizontal and vertical dipoles spaced at 10 m intervals, suggesting fractured zones (conductive zones) or thickness-weathered layers. With conductivity values ranging from 18 to 107 mS/m in Figure 8 (a and b), which is suggestive of a worn zone, necking was seen across the profile on the horizontal and vertical dipole with 10 and 20 m spacing.

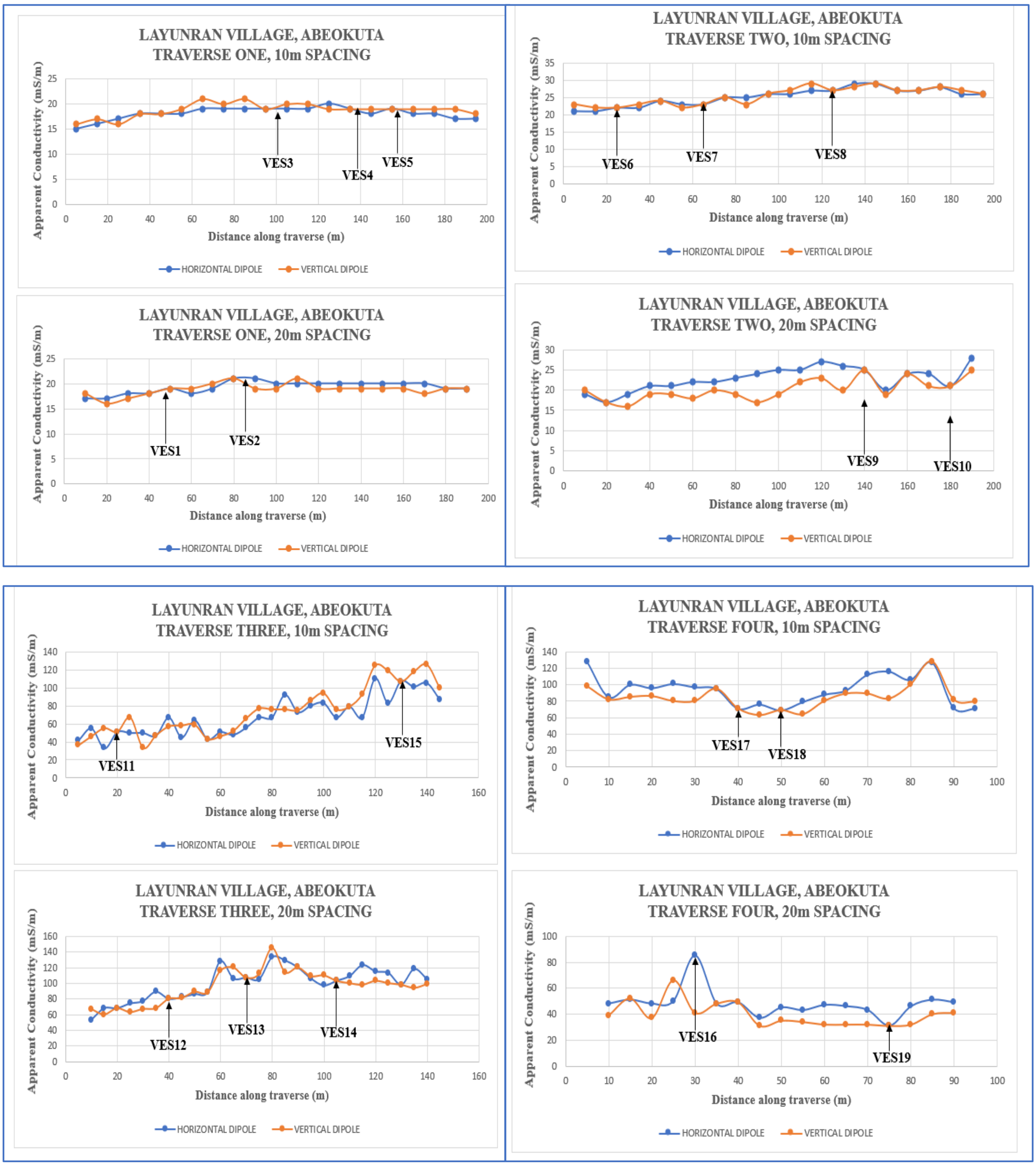

Figure 8a: EM34 Plot along Traverse 1 – 4.

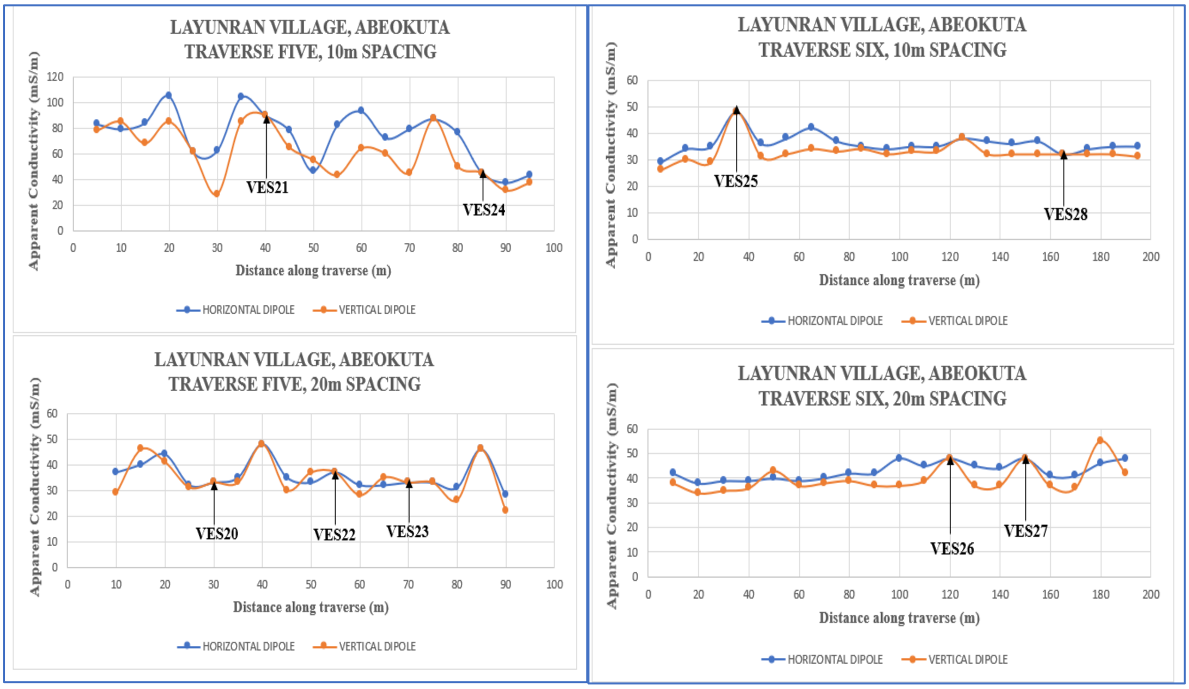

Figure 8b: EM34 Plot along Traverse 5 – 6.

The areas of anomalous response for the EM correlate with the weathered/fractured basement region observed beneath the VES point. Also, the combination of electromagnetic and electrical resistivity shows distinct conductivity and resistivity signatures and the versatility of the methods in delineating the fractured/weathered basement layer that constitutes hydrogeologic units where groundwater can be tapped.

CONCLUSION

Layunrun Village, a typical basement complex in Ogun State, Nigeria, has its groundwater potentiality investigated using electrical resistivity and electromagnetic methods. Analysis and the creation of thematic maps of the region were done using the VES curves produced using the traditional partial curve matching. These findings were combined with those from the electromagnetic data. Within the study area, between four and six geoelectric layers were found. Topsoil, weathered layer (clay), weathered layer, fractured basement, and fresh basement are the layers that these terms refer to. The findings indicate that the overburden thickness ranges from 9 to 17 m in the majority of the area, with a maximum overburden of 23 m. The study area is well fractured, with fracture thicknesses ranging from 12 to more than 30 m. The basement topography is undulating, with more depressions in the western and central parts of the study area, which may act as areas where groundwater collects. These findings and the electromagnetic findings have a good correlation. These indicate that the Layunrun hamlet has good potential for groundwater accumulation, and as a result, borehole drilling techniques could be used to develop groundwater by utilizing zones with substantial overburden and fracture columns to supply potable water for the locals. The findings also suggested that a town with similar geology beneath it may use electromagnetic and electrical resistivity methods to find regions with good groundwater potentials.

REFERENCES

Agagu, O.K. (1985). A geological guide to bituminous sediments in Southwestern Nigeria. Unpublished Report, Department of Geology, University of Ibadan

Ariyo, S. and Adeyemi, G. (2012). Geo-electrical characterization of aquifers in the basement complex/ sedimentary transition zone Southwestern Nigeria. Int J Adv Sci Res Technol 2:1

Bhattacharya, A.P.K. and Patra, H.P. (1968). Direct Current Geoelectric Sounding: Principles and Interpretations: Methods of Geochemistry and Geophysics. Elsevier Publishing Company, Amsterdam. 135.

Klein, J. and Lajoie, J. (1980). Electromagnetic Prospecting for minerals. Practical geophysics for the Exploration geologists. Northwest Mining Association, Spokane, WA: 239 -290

Kumar, A., Tiwari, R.K., Routh, P.S., and Pandey, A. (2018). Integrated geophysical investigations for mapping subsurface aquifers in agricultural fields. Environmental Earth Sciences, 77(2), 60.

Madramootoo, C.A., and Fyles, H. (2018). Climate change and implications for water management on agricultural lands. Canadian Journal of Soil Science, 98(2), 139-156.

Milsom, J. (1996). Field Geophysics, 2nd ed. 187 pp. Chichester, New York, Brisbane, Toronto, Singapore: John Wiley & Sons. ISBN 0 471 96634 7.

Minsley, B.J., Ajo-Franklin, J.B., Revil, A. and Hubbard, S.S. (2015). Electromagnetic methods in applied geophysics—Theory. In Treatise on Geophysics (2nd ed., Vol. 7, pp. 71-140). Elsevier.

Ritz, M., Jean-Claude Parisot, Diouf, S.A., Beauvais, S., Dione, F. and M. Niang, M. (1999). Electrical imaging of lateritic weathering mantles over granitic and metamorphic basement of eastern Senegal, West Africa. Journal of Applied Geophysics, 41, 335–344.

Saha, A.K., Roy, S. and Bhattacharya, P. (2019). Hydrogeophysical investigation for failed borehole and detection of deep fracture zones: A case study in India. Journal of Earth System Science, 128(3), 67.

Van Nostrand, R.G. and Cook, K.L. (1966). Interpretation of Resistivity Data. United States Government Printing Office, Washington.

Yan, J. and Zhang, X. (2016). An improved airborne electromagnetic method for detecting groundwater in coastal areas. Environmental Earth Sciences, 75(6), 495.